Spatial degradation of pulse contrast in the focal plane for pulsed laser beams from chirped-pulse amplification system

Qingwei Yang [a],*, Mingwei Liu [b], Yanhai Wang [c], Xinglong Xie [a], Ailin Guo [a], Zunqi Lin [a]

[a] National Laboratory on High Power Laser and Physics, Shanghai Institute of Optics and Fine Mechanics, Chinese Academy of Sciences, No. 390, Qinghe Road, Jiading District, Shanghai 201800, China
[b] School of Physics, Hunan University of Science and Technology, Hunan 411201, China
[c] College of Sciences, Hebei University of Science and Technology, Shijiazhuang 050018, China

ARTICLE INFO

ABSTRACT

A two-dimension model is presented to analyze the spatial dependence of pulse contrast in the focal plane. The parameters of the SHENGUANG (SG) II laser system are demonstrated as examples. Comparing with the degradation in the beam centroid, the pulse contrast degrades more seriously in the transverse. This spatial degradation of pulse contrast can be improved, such as by controlling the spatial spectrum clipping.

1. Introduction

The chirped pulse amplification (CPA) technique [1,2] is commonly used to build up high power laser systems for kinds of experiments and applications, such as laser-driven plasma accelerators [3,4] and inertial confinement fusion [3,5]. The peak laser intensity up to 10^{22} W/cm^2 is now achievable and is expected to boost to 10^{24} W/cm^2 in the near future [6]. However, the pulse contrast is typically about 10^7–10^8. That is, prepulses with intensity more than 10^{14} W/cm^2 may be generated before the main pulse, while the 10^{10} W/cm^2 prepulse is strong enough to produce preplasma and modify the target conditions.

The pulse contrast is usually calculated (as well as measured in experiments) just after the compressor [7–10], implying that the spectrum is transversely (spatially) uniform. However, a pulsed laser beam out of the compressor has to be focused on the target in the experiments of laser–matter interactions. Correspondingly, the spectrum distribution in the focal plane is nonuniform and depends on the spatial distribution. To our knowledge, there is no analysis on this kind of spatial dependence of pulse contrast.

In this article, we present a model to analyze the pulse contrast in the focal plane. Making use of the parameters of the SG II laser system, the pulse contrast is demonstrated to degrade with the position away from the beam centroid in the focal plane.

2. Model

The pulse contrast is associated with the temporal distribution of the normalized laser intensity. It is well-known that focusing a laser beam by an off-axis parabolic (OAP) mirror can be expressed in terms of the Fraunhofer-diffraction. The input function of the OAP mirror should be determined by the whole CPA system and the subsequent propagation in free space, while the influence from the latter is negligible. Then the spectrum function in the focal plane (ξ, η) simply reads

$$A_f(\omega, \xi, \eta) = F^{-1}[A_0(\omega, x, y)] \tag{1}$$

where F^{-1} denotes the inverse Fourier transform, $f_x = \xi/\lambda f$ and $f_y = \eta/\lambda f$ are the spatial frequencies, λ is the laser wavelength, f is the focal length of the OAP mirror, and $A_0(\omega, x, y)$ is the spectrum function out of the compressor. The laser intensity in the focal plane is then given by

$$I(t, \xi, \eta) = \left| \frac{1}{2\pi} \int_{\omega_1}^{\omega_2} A_f(\omega, \xi, \eta) \exp[-i\omega t] d\omega \right|^2, \tag{2}$$

* Corresponding author.
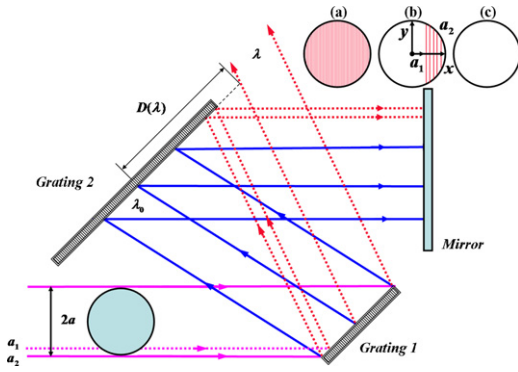E-mail address: yqwphy@siom.ac.cn (Q. Yang).

Fig. 1. The sketch of a grating compressor. In the cases of different spectral clipping, the spatial spectrum distribution in the compressor output plane is shown with the insets (a)–(c).

where $\omega_1 = 2\pi c/\lambda_1$, $\omega_2 = 2\pi c/\lambda_2$, λ_1 and λ_2 are the maximum and the minimum values of λ determined by the laser system, and c is the speed of light in vacuum.

In general, the expression of $A_0(\omega, x, y)$ can be further written as

$$A_0(\omega, x, y) = A_t(\omega)A_s(x, y), \tag{3}$$

where

$$A_t(\omega) = E(\omega)\sqrt{\varepsilon_g(\omega)}\exp[i\phi(\omega)] \tag{4}$$

is related to the temporal spectrum distribution, $E(\omega)$ is the spectrum amplitude, $\varepsilon_g(\omega)$ is the total diffraction efficiency of the gratings, $\phi(\omega)$ is the total residual phase of the laser system, and $A_s(x, y)$ describes the spatial distribution. Eq. (2) reduces to be

$$I(t, \xi, \eta) = \left| \frac{1}{2\pi} \int_{\omega_1}^{\omega_2} A_f(\omega)\exp[-i\omega t]d\omega \right|^2,$$

i.e., the model used in the previous analysis of pulse contrast [3,11,12], in the absence of beam focusing.

In the presence of beam focusing [i.e., Eq. (2)], the pulse contrast in the focal plane is spatially dependent, as indicated in Eqs. (1) and (3). This spatial dependence should be determined by the whole laser system, such as the spectral clipping, residual phase, and diffraction efficiency of the gratings. However, for the sake of simplicity, only the effect of spectral clipping from the compressor is analyzed as examples in the following.

A grating compressor is typically as that plotted in Fig. 1. The Grating 1 and Grating 2 are the first and the second gratings, while "Mirror" denotes the reflection mirror. The insets (a)–(c) in Fig. 1 plot the situations of spectrum clipping for a certain wavelength through the compressor. The widths of the first and the second gratings are W_a and W_b, respectively. The clipping function is given by $D(\lambda) = L \cos \beta(\lambda_0)[\tan \beta(\lambda) - \tan \beta(\lambda_0)]$, where $\beta(\lambda)$ is the wavelength-dependent diffraction angle and satisfies the grating equation $\sin \gamma + \sin \beta(\lambda) = \lambda N$, γ is the incident angle on the first grating, λ_0 is the central wavelength, N is the grating line density, $L = c\lambda_0 C_R \cos^2 \beta(\lambda_0)/(\lambda_0 N)^2$, and C_R is the chirped ratio of the compressor. The spatial profile of the (compressor) input beam is assumed to be top-hat with radius a, i.e., $A_i(x, y) = circ(\rho/a)$, where $\rho = \sqrt{x^2 + y^2}$ and $circ(x)$ denotes the circle function.

Usually, the width of the first grating is assumed to be larger enough to reflect all of the spectrum components. That is, the spatial function $A_s(x, y)$ mainly relays on the width of the second grating. For example, when $|D(\lambda)| \leq (W_b - W_a)/2$, all of the spectrum components can be exported from the compressor, as shown with the inset (a) in Fig. 1. The spatial distribution function is then given by $A_s(\omega, x, y) = circ(\rho/a)$, i.e., one has

$$A_f(\omega, \xi, \eta) = \frac{A_t a^2 J_1(2\pi\chi)}{\chi}, \tag{5}$$

where $\chi = a\sqrt{f_x^2 + f_y^2}$ and $J_1(x)$ denotes the Bessel function of the first kind.

The clipping function is also wavelength-dependent. When the value of the clipping function satisfies the relation $(W_b - W_a)/2 < |D(\lambda)| < (W_b + W_a)/2$, i.e., there is partial spectrum clipping [as shown with the inset (b) in Fig. 1], the spatial distribution function should be written as

$$A_s(\omega, x, y) = \begin{cases} 1, & \text{for } \rho \leq a \text{ and } a_1 \leq x \leq a_2 \\ 0, & \text{otherwise} \end{cases} \tag{6}$$

where a_1 and a_2 are the displacements associated with the spectrum clipping: if $D(\lambda) < 0$, one has $a_1 = -[W_b/2 + D(\lambda)]\cos \gamma$ and $a_2 = a$; otherwise, one has $a_1 = -a$ and $a_2 = [W_b/2 - D(\lambda)]\cos \gamma$. Substituting Eqs. (6) and (4) into Eq. (1), yields

$$A_f(\omega, \xi, \eta) = A_t \int_{a_2}^{a_1} \exp[-i2\pi f_x x]\frac{\sin(2\pi f_y \sigma)}{\pi f_y}dx, \tag{7}$$

where $\sigma = \sqrt{a^2 - x^2}$. Moreover, for some spectral components, the value of W_b is so small that $|D(\lambda)| > (W_b + W_a)/2$. Then there is full spectrum clipping, i.e.,

$$A_f(\omega, \xi, \eta) = 0, \tag{8}$$

as shown with the inset (c) in Fig. 1. For a given compressor, the expression of $A_f(\omega, \xi, \eta)$ is then determined by the value of $D(\lambda)$, i.e., Eqs. (5), (7) and (8).

3. Numerical results

To demonstrate the spatial dependence of pulse contrast in the focal plane, we take the parameters used in the SG II laser system [5] as examples. The chirped ratio is $C_R = 3.2$ ns/6.5 nm, making use of multi-layer dielectric gratings with $N = 1740$ mm^{-1}. The widths of the gratings are $W_a = 940$ mm and $W_b = 1220$ mm. The incidence angle is $\gamma = 70°$. The spot size of the input laser beam is $a = 160$ mm. The central wavelength is $\lambda_0 = 1053$ nm, while the minimum and the maximum values are $\lambda_1 = 1043.5$ nm and $\lambda_2 = 1062.5$ nm. The focal length of OAP mirror is $f = 800$ mm. For simplicity, we neglect the influence of the residual phase and the diffraction efficiency is assumed to be uniform, i.e., $\phi(\omega) = 0$ and $\varepsilon_g(\omega) = 1$. Moreover, the pulse out of the compressor is assumed to be expressed with the fundamental Gaussian function. Eq. (4) then can be written as

$$A_t(\omega) = \exp\left[-\frac{\tau^2(\omega - \omega_0)^2}{8 \ln 2}\right], \tag{9}$$

where $\omega_0 = 2\pi c/\lambda_0$ and $\tau = 0.5$ ps is the pulse width (FWHM, full width at half maximum).

Without considering the spatial dependence, i.e., assuming uniform spatial distribution in the focal plane, the (theoretical) pulse contrast shows an ideal case, as the black curve plotted in Fig. 2(a). In the presence of beam focusing [i.e., Eqs. (2), (5) and (7)–(9)], the pulse contrast shows strongly spatial dependence in the focal plane, as the color curves plotted in Fig. 2(a). Here I_r is the laser intensity at the radius $r = \sqrt{\xi^2 + \eta^2}$ in the focal plane, $I_{r0} = I_r(t=0)$ is the corresponding maximum value, and $D_L = 1.22\lambda_0 f/a$ is the diffraction limit. Comparing with the ideal case, the pulse contrast degrades almost three orders of magnitude within few picoseconds before the main pulse even in the beam centroid, as the blue curve shown in Fig. 2(a). This degradation is enhanced with the increase
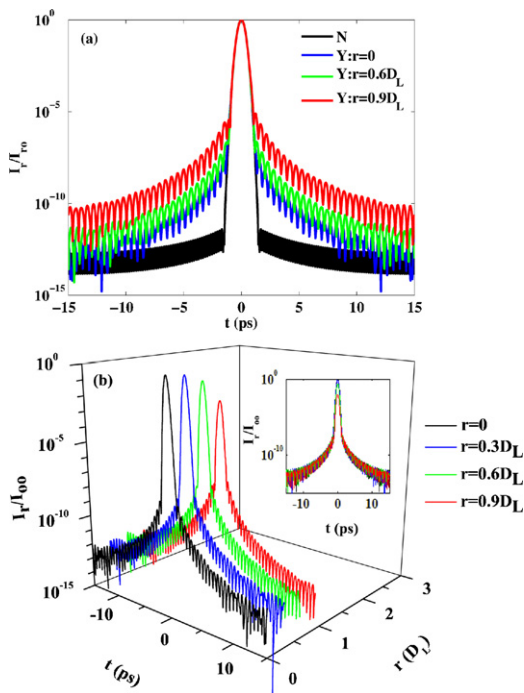
Fig. 2. (a) The temporal distribution of the laser intensity (normalized by I_{r0}) in the cases of considering the spatial degradation (Y) or not (N). (b) The distribution of the laser intensity (normalized by I_{00}, the value in the beam centroid) in the focal plane. (For interpretation of the references to color in the text, the reader is referred to the web version of the article.)
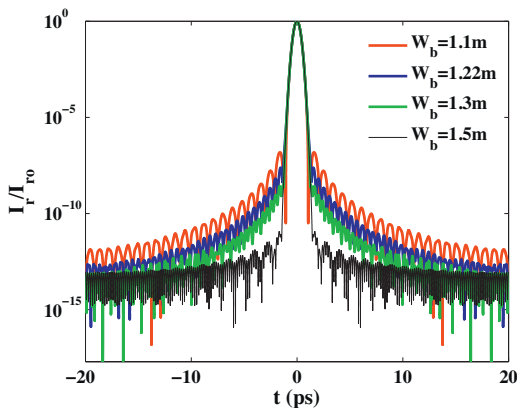

Fig. 3. The temporal distribution of the normalized laser intensity in the cases of different widths of the second grating. Other parameters are the same as those used in Fig. 1. (For interpretation of the references to color in the text, the reader is referred to the web version of the article.)

of the radius in the focal plane. For example, the degradation of pulse contrast up to six orders of magnitude occurs when $r = 0.9D_L$, as the red curve shown in Fig. 2(a). What should be mentioned is that the realistic beam spot size is often several times of D_L in the focal plane. Therefore, in the case of beam focusing, the pulse contrast may depend seriously on the spatial distribution in the focal plane, as indicated in Eqs. (1) and (2).

However, a laser beam, e.g., with Gaussian transverse distribution, in general is most intense in the beam centroid. That is, for the effective pulse contrast at a given radius r in the focal plane, one needs to consider both the effects of transverse intensity decrease and spatial pulse contrast degradation. The laser intensities plotted in Fig. 2(b) are normalized by the value $I_{00} = I(r = 0, t = 0)$, i.e., the maximum intensity in the beam centroid. It is seen that the

(normalized) laser intensities I_r/I_{00} present almost the same except their maximum values. Therefore, the laser transverse distribution in the pulse front is top-hat-like in the focal plane, due to the spatial degradation of pulse contrast.

According to Eqs. (1) and (7), the pulse contrast tends to be more strongly dependent on the spatial expression of $A_f(\omega, \xi, \eta)$ in the presence of spectrum clipping, which arises from the finite size of the second grating. In Fig. 3, we vary the value of W_b, while other parameters are the same as those used in Fig. 2. In the beam centroid, i.e., Fig. 3 with $r = 0$, the pulse contrast further degrades when W_b decreases from 1.22 m to 1.1 m. On the contrary, the spatial degradation can be improved with larger value of W_b, such as the green curve in Fig. 3 shows. When the value of W_b is large enough, e.g., $W_b = 1.5$ m (the black curve plotted in Fig. 3), the distribution of the laser intensity tends to be similar to the ideal case without considering beam focusing (without shown). Then the degradation of pulse contrast in the beam centroid is negligible.

4. Conclusion

In summary a two-dimension model is presented to analyze the pulse contrast in the focal plane. The pulse contrast degrades even in the beam centroid due to beam focusing. This degradation enhances with the increase of the radius in the focal plane. Increasing the width of the second grating in the compressor is helpful to improve the spatial degradation of pulse contrast, especially in the beam centroid.

References

[1] E.B. Treacy, Optical pulse compress with diffraction gratings, IEEE J. Quantum Electron. QE-5 (9) (1969) 454–458.
[2] D. Strickland, G. Mourou, Compression of amplified chirped optical pulses, Opt. Commun. 56 (3) (1985) 219–222.
[3] G.A. Mourou, T. Tajima, S.V. Bulanov, Optics in the relativistic regime, Rev. Mod. Phys. 78 (2) (2006) 309–371.
[4] K. Nakajima, Compact X-ray sources: towards a table-top free-electron laser, Nat. Phys. 4 (2008) 92–93.
[5] G. Xu, T. Wang, Z. Li, Y. Dai, Z. Lin, Y. Gu, J. Zhu, 1 kJ petawatt laser for SG-II-U program, Rev. Laser Eng. (Suppl. Vol.) (2008) 1172–1175.
[6] A. Jullien, O. Albert, F. Burgy, G. Hamoniaux, L.P. Rousseau, J.P. Chambaret, F. Auge-Rochereau, G. Cheriaux, J. Etchepare, N. Minkovski, S.M. Saltiel, 10^{-10} temporal contrast for femtosecond ultraintense lasers by cross-polarized wave generation, Opt. Lett. 30 (8) (2005) 920–922.
[7] H. Ren, L. Qian, H. Zhu, D. Fan, P. Yuan, Pulse-contrast degradation due to pump phase-modulation in optical parametric chirped-pulse amplification system, Opt. Express 18 (2010) 12948–12959.
[8] C. Liu, Z. Wang, W. Li, Q. Zhang, H. Han, H. Teng, Z. Wei, Contrast enhancement in a Ti: sapphire chirped-pulse amplification laser system with a non-collinear femtosecond optical parametric amplifier, Opt. Lett. 35 (18) (2010) 3096–3098.
[9] Y. Huang, C. Zhang, Y. Xu, D. Li, Y. Leng, R. Li, Z. Xu, Ultrashort pulse temporal contrast enhancement based on noncollinear optical-parametric amplification, Opt. Lett. 36 (6) (2011) 781–783.
[10] S. Fourmaux, S. Payeur, S. Buffechoux, P. Lassonde, C. St-Pierre, F. Martin, J.C. Kieffer, Pedestal cleaning for high laser pulse contrast ratio with a 100 TW class laser system, Opt. Express 19 (9) (2011) 8486–8497.
[11] M. Trentelman, I.N. Ross, C.N. Danson, Finite size compression gratings in a large aperture chirped pulse amplification laser system, Appl. Opt. 36 (33) (1997) 8567–8573.
[12] B.C. Li, W. Theobad, E. Welsch, R. Sauerbrey, Optimization of grating size in chirped-pulse-amplification laser system, Appl. Phys. B 71 (2000) 819–826.